doi:10.1017/S1431927621007017
Microsc. Microanal. 27 (Suppl 1), 2021

Transmission ion microscopy and time-of-flight spectroscopy

Michael Mousley[1], Wolfhard Moeller[2], Patrick Philipp[1], Olivier Bouton[1], Nico Klingner[3], Eduardo Serralta[3], Gregor Hlawacek[4], Tom Wirtz[5] and Santhana Eswara[1]

[1]Luxembourg Institute of Science and Technology, Belvaux, Luxembourg, [2]Helmholtz-Zentrum Dresden-Rossendorf, dresden, Germany, [3]Helmholtz-Zentrum Dresden-Rossendorf, United States, [4]Helmholtz-Zentrum Dresden-Rossendorf, Dresden, Sachsen, Germany, [5]Luxembourg Institute of Science and Technology (LIST), Belvaux, Luxembourg

A Transmission Ion Microscope (TIM), the Galileo prototype, has been built at the Luxembourg Institute of Science and Technology (LIST) [1]. This is part of a new interest in the imaging properties of transmitted helium ions [2] [3] [4]. This allows the combination of both helium ions and neutrals to be detected after passing through a sample, or, if post sample deflection is used, then only the signal from the neutrals (Figure 1 A). The helium ions have an energy between 10 keV and 20 keV and are produced in a Duoplasmatron ion source.

The prototype instrument is very flexible and uses a microchannel plate (MCP) which can be configured in multiple ways to enable analysis modalities, producing datasets of varying dimensionality. 2D images can be obtained either with a phosphor screen and a defocussed beam in direct TIM mode (analogous to transmission electron microscopy) or with an anode plate to collect the total detector signal in scanning mode providing scanning-TIM (STIM) images. By using fast blanking electronics (similar to [5]), pulses of ions can be used to add time-of-flight (TOF) information, allowing a TOF-STIM mode to collect 3D datasets (x, y, t). Alternatively, a delay line detector (DLD) can be used to provide detector plane images with corresponding TOF values at each detector pixel, to collect TOF-TIM 3D datasets (x', y', t). Finally, detector imaged DLD TOF-STIM can be used, in this mode, for each beam position on the sample, the arrival time and position on the detector is recorded for each count (5D datasets, x, y, x', y', t). The prototype TIM is also equipped with a secondary electron (SE) detector providing additional SE intensity for each pixel position in STIM modes (Figure 1 B).

Example TOF datasets from materials science related samples (e.g. Au on Si) will be presented. In addition to microscopy, the effects of 20 keV helium ion irradiation on Au-Silica core-shell nanoparticles have been evaluated. Using bright field Transmission Electron Microscopy (TEM) imaging of irradiated particles, the effects of irradiation were tracked for increasing fluences [6]. It was seen that satellite particles are formed around the main Au core (Figure 2, A and B) and neighbouring silica shells fuse together (Figure 2, C and D). These effects will determine the suitable fluences when imaging nanoparticles with 20 keV helium ions.

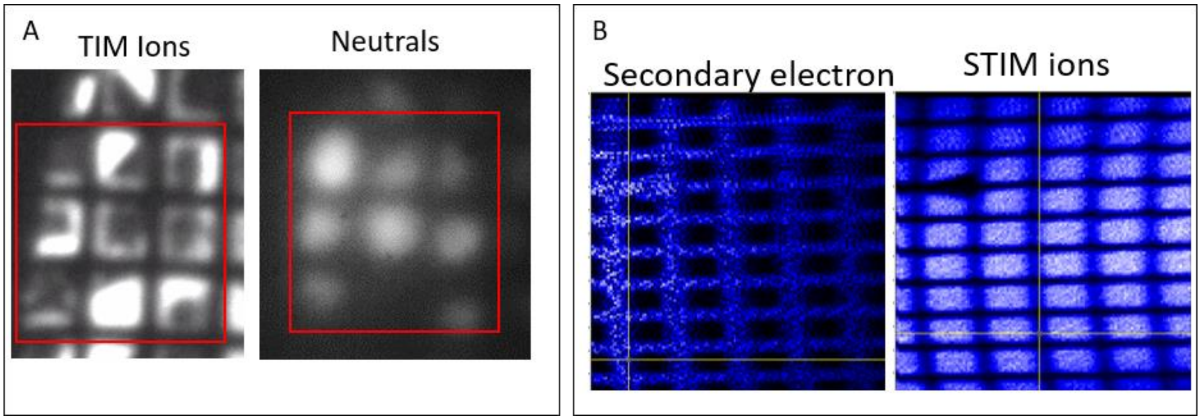

Figure 1. A) TIM images formed with ions and neutrals the sample is 300-mesh lacey carbon grid covered with a single layer graphene membrane, pitch 85 µm (31 µm bar, 54 µm hole). B) Secondary electron and STIM images recorded concurrently in scanning mode (using MCP/anode plate detection).

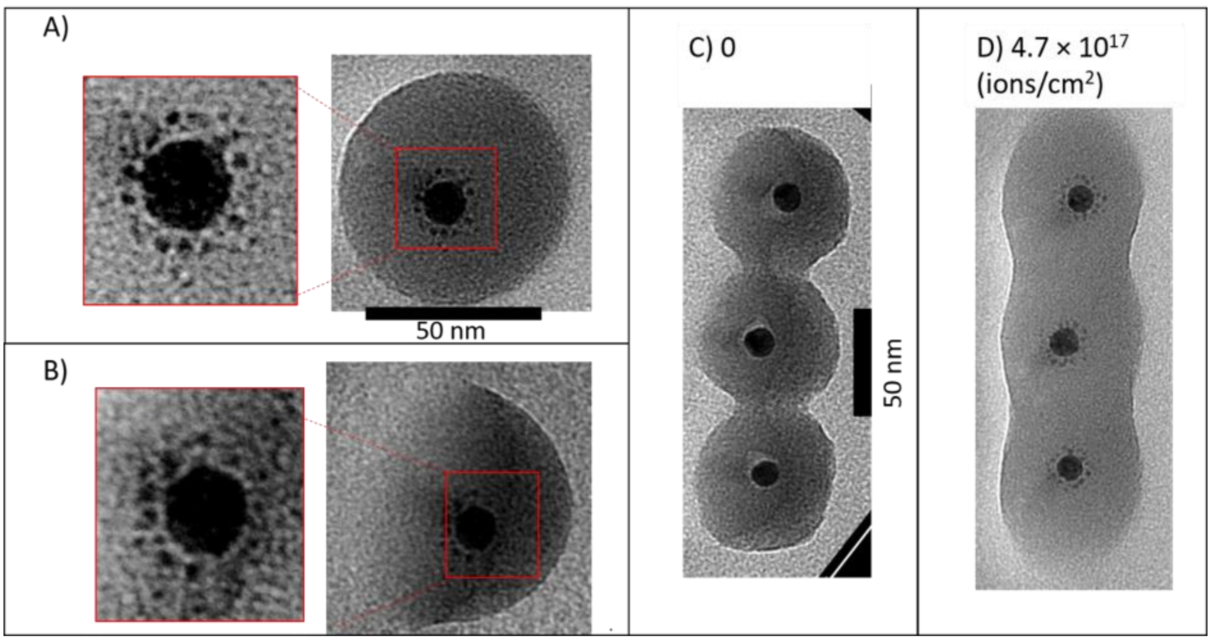

Figure 2. Bright field TEM images at 0 degrees tilt (A) and 60 degrees tilt (B) of a core-shell particle after 4.7x1017 ions/cm2. Bright field TEM images of a collection of core-shell particles before (C) and after (D) 4.7x1017 ions/cm2 20 keV helium ion irradiation.

References

[1] M. Mousley *et al.*, "Stationary beam full-field transmission helium ion microscopy using sub-50 keV He+: Projected images and intensity patterns," *Beilstein J. Nanotechnol.*, vol. 10, pp. 1648–1657, Aug. 2019, doi: 10.3762/bjnano.10.160. [Online]. Available: https://www.beilstein-journals.org/bjnano/articles/10/160

[2] K. L. Kavanagh C. Herrmann and J. A. Notte, "Camera for transmission He $^{+}$ ion microscopy," *J. Vac. Sci. Technol. B, Nanotechnol. Microelectron. Mater. Process. Meas. Phenom.*, vol. 35, no. 6, p.

06G902, 2017, doi: 10.1116/1.4991898. [Online]. Available: http://avs.scitation.org/doi/10.1116/1.4991898
[3] T. Wirtz O. De Castro J.-N. Audinot and P. Philipp, "Imaging and Analytics on the Helium Ion Microscope," *Annu. Rev. Anal. Chem.*, vol. 12, no. 1, 2019, doi: 10.1146/annurev-anchem-061318-115457.
[4] E. Serralta *et al.*, "Scanning transmission imaging in the helium ion microscope using a microchannel plate with a delay line detector," *Beilstein J. Nanotechnol.*, vol. 11, pp. 1854–1864, 2020, doi: 10.3762/BJNANO.11.167.
[5] N. Klingner R. Heller G. Hlawacek S. Facsko and J. von Borany, "Time-of-flight secondary ion mass spectrometry in the helium ion microscope," *Ultramicroscopy*, vol. 198, no. March 2019, pp. 10–17, 2019, doi: 10.1016/j.ultramic.2018.12.014. [Online]. Available: https://doi.org/10.1016/j.ultramic.2018.12.014
[6] M. Mousley *et al.*, "Structural and chemical evolution of Au-silica core–shell nanoparticles during 20 keV helium ion irradiation: a comparison between experiment and simulation," *Sci. Rep.*, vol. 10, no. 1, pp. 1–13, 2020, doi: 10.1038/s41598-020-68955-7. [Online]. Available: https://doi.org/10.1038/s41598-020-68955-7